

# Journal of Photonics for Energy

SPIEDigitalLibrary.org/jpe

## **Influence of point defects on the performance of InVO<sub>4</sub> photoanodes**

Roel van de Krol  
Julie Ségalini  
Cristina S. Enache

# Influence of point defects on the performance of InVO<sub>4</sub> photoanodes

Roel van de Krol, Julie Ségalini, and Cristina S. Enache

Delft University of Technology, Faculty of Applied Sciences, Department of Chemical Engineering/ Materials for Energy Conversion and Storage, P.O. Box 5045, 2600 GA Delft, The Netherlands  
[r.vandekrol@tudelft.nl](mailto:r.vandekrol@tudelft.nl)

**Abstract.** The properties of thin film InVO<sub>4</sub> photoanodes for water splitting have been studied. Compact films of InVO<sub>4</sub> were prepared by spray pyrolysis and are found to be stable between pH 3 and 11. Although the indirect bandgap is 3.2 eV, a modest amount of visible light absorption is observed. The origin of this absorption is attributed to the presence of deep donor states at ~0.7 eV below the conduction band. These donor states presumably correspond to oxygen vacancies, which form as a result of small but unavoidable deviations of In:V from the ideal 1:1 stoichiometry during the wet-chemical synthesis process. Shallow donors are absent in this material, in contrast to what is normally observed for metal oxides. The deep donor model explains the much stronger visible light absorption of powders compared to thin films. The defect chemical reactions that lead to the formation of the deep donors are shown, and are supported by photoluminescence data. © 2011 Society of Photo-Optical Instrumentation Engineers (SPIE). [DOI: [10.1117/1.3564926](https://doi.org/10.1117/1.3564926)]

**Keywords:** InVO<sub>4</sub>; photoelectrochemistry; photoanode; water splitting; defect chemistry; photoluminescence.

Paper 10165PR received Sep. 29, 2010; revised manuscript received Jan. 17, 2011; accepted for publication Feb. 21, 2011; published online Mar. 17, 2011.

## 1 Introduction

Solar water splitting for clean, renewable production of hydrogen is an appealing prospect in view of the growing environmental concerns associated with conventional energy sources. Compared to coupled photovoltaic-electrolysis systems, direct photoelectrolysis with semi-conducting photoelectrodes offers the benefit of lower systems costs, and possibly also higher efficiencies.<sup>1</sup> While current state-of-the-art systems based on sophisticated multi-junction devices combine solar-to-hydrogen (STH) efficiencies of up to 18% with excellent stability against photocorrosion,<sup>2</sup> they are too expensive for large-scale terrestrial application.<sup>3</sup> Low-cost transition metal oxides may represent an attractive alternative. Recent breakthroughs in the synthesis of nanostructured electrodes show that STH efficiencies of 2.2% (for  $\alpha$ -alpha Fe<sub>2</sub>O<sub>3</sub>) and 3.6% (for WO<sub>3</sub>) are now within reach when using a tandem cell configuration.<sup>4,5</sup>

Despite these advances, no metal oxide has yet been found that combines the three main requirements for water splitting, i.e., good visible light absorption, high photochemical stability, and suitable band energetics so that no additional bias voltage is required. After more than three decades of intensive research on many different undoped and doped oxides, one may tentatively conclude that; i. no binary oxide can split water with appreciable efficiencies unless a tandem cell approach is used, and ii. doping wide-bandgap oxides to enhance the visible-light response does not result in higher overall efficiencies. The latter is due to the concomitant increase in recombination when optically active deep donors or acceptors are introduced.

In view of these considerations, many efforts are now geared toward ternary and even more complex metal oxides. These efforts are motivated by the numerous possible compositions and the fact that only a handful of these have been studied as water splitting photocatalysts. In this paper, we explore the properties of InVO<sub>4</sub> photoelectrodes. As shown by Ye et al. in their work on InVO<sub>4</sub> powders, it is one of the few oxides that shows hydrogen evolution from pure water under visible light illumination.<sup>6</sup> This clearly indicates that the conduction band minimum is more negative than the hydrogen evolution potential, one of the key requirements for water splitting without assistance of a bias potential. Porous InVO<sub>4</sub> electrodes also show a visible-light photoresponse, although the photocurrents are relatively low.<sup>7</sup> Despite several other reports on this material,<sup>8,9</sup> little is known about the intrinsic material properties and the factors that limit its photocatalytic and/or photoelectrochemical performance.

We have recently shown that it is possible to make thin, compact films of (nearly) phase-pure orthorhombic InVO<sub>4</sub> at low temperatures (<600°C) by using spray pyrolysis.<sup>10</sup> The bandgap of InVO<sub>4</sub> was found to be significantly larger than suggested by previous reports, and deep donor states were found to be responsible for the visible light absorption of the material. In this paper, we report on the chemical stability of InVO<sub>4</sub> and we provide additional optical evidence for the presence of the deep donor states.

## 2 Experimental

InVO<sub>4</sub> thin films were prepared by spray pyrolysis of an ethanolic precursor solution onto a heated substrate in air. The precursor solution consisted of In(NO<sub>3</sub>)<sub>3</sub> (99.99%, Alfa Aesar) and VCl<sub>3</sub> (99%, Alfa Aesar) dissolved in ethanol (>99.9%, J.T. Baker). After the metal salts were dissolved in ethanol, the nitrate groups from the indium precursor rapidly oxidize the V<sup>3+</sup> ions (green) to V<sup>4+</sup> (purple), followed by a much slower overnight oxidation to V<sup>5+</sup> (yellow). This solution is stable for several months after preparation. The total concentration was 0.2 M, and an In/V ratio of 1:1 was used. Nitrogen was used as a carrier gas, and the substrate temperature was 400°C (measured by pressing a small thermocouple to the sample surface). A 5-s on -120-s off spraying cycle was used to allow the solvent to evaporate before depositing the next layer. The films were deposited onto 1-mm thick fused silica substrates (Heraeus, Suprasil 1 quartz) for optical characterization, and onto transparent conducting glass (FTO, 15 Ω/sq. F-doped SnO<sub>2</sub>, TEC-15, Libbey Owens-Ford) for photoelectrochemical studies. All films were subjected to a postdeposition thermal anneal at 550°C in air for 6 h in order to further improve the stoichiometry and crystallinity. InVO<sub>4</sub> powders were synthesized by ball milling of In<sub>2</sub>O<sub>3</sub> (Alfa Aesar 99.99%) and V<sub>2</sub>O<sub>5</sub> (Alfa Aesar 99.9%) powders. Stoichiometric amounts of the powders were introduced in a zirconium oxide ball-milling jar of 12 ml containing 6 zirconium oxide balls of 10 mm of diameter. The oxide powders were milled in a Fritsch Pulverisette 5 planetary ball mill during 5 h at 400 rpm. The resulting powder was fired at 800°C in air for 12 h, after which 6-mm pellets were pressed using a pressure of ~270 MPa. This was followed by another thermal anneal at 800°C in air for 2 h to yield mechanically stable, bright yellow pellets.

Optical transmission and reflection spectra of the thin InVO<sub>4</sub> films were recorded using a Perkin-Elmer Lambda 900 spectrophotometer equipped with an integrating sphere (Labsphere). The morphology of the films was characterized using a high-resolution scanning electron microscope equipped with a field emission gun (Philips XL-SFEG). Luminescence spectra were recorded with a Quanta-Master QM-1 fluorimeter.

Photoelectrochemical experiments were performed in a conventional three-electrode cell with a quartz window, a platinum counter electrode, and an Ag/AgCl reference electrode (3 M KCl, REF 321, Radiometer Analytical). A solution of 0.1 M KOH (J.T. Baker) in demineralized and deionized water (Milli-Q, 18.2 MΩ cm) was used as the electrolyte. Nitrogen gas was bubbled through the solution to remove any dissolved oxygen. Electrical contacts to InVO<sub>4</sub>/FTO were made by connecting copper wires to the conducting substrate with silver paint (Bison Electro) or with graphite paint. The contact was covered with an epoxy resin to improve mechanical

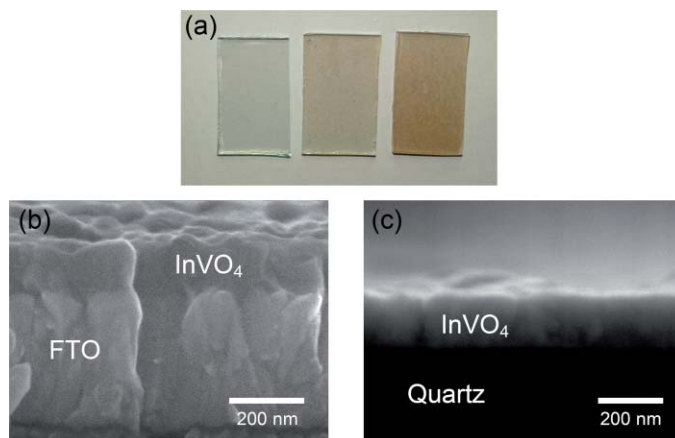


**Fig. 1** (a) Photograph of an uncoated FTO substrate (left) and two InVO<sub>4</sub> films with increasing thickness (middle, right). SEM micrographs of spray-deposited InVO<sub>4</sub> films on FTO glass (b), and on quartz (c).

stability. The working area of the electrodes exposed to the electrolyte was  $2.83 \times 10^{-5} \text{ m}^2$  (6-mm diameter) for all samples. Potential control was provided by an EG&G model 283 potentiostat. A 200 W tungsten halogen lamp in combination with a grating monochromator (Acton SPro 150) was used to irradiate the sample. High-pass filters (Schott) were used to remove the second order of the diffracted light. The light source for AM1.5 measurements was a solar simulator (EPS 1200S, KH Steuernagel Lichttechnik GmbH). Photocurrent voltammograms were recorded using 375 nm light emitting diodes (LEDs) (Roithner, type LED375-06, 2.5 mW) as a monochromatic light source. The light intensity was measured as a function of wavelength with a calibrated photodiode (PD 300-UV, Ophir). Photocurrent action spectra were recorded using a lock-in amplifier (EG&G PAR model 5210) connected to the potentiostat.

### 3 Results and Discussion

Spray deposition at 400°C, followed by a thermal anneal at 550°C yields yellow-brownish films that are homogeneous and crack-free (Fig. 1). The films adhere well to the FTO substrate, and cannot be removed by a Scotch-tape test. Edge-on scanning electron microscopy (SEM) thickness analysis reveals a typical thickness between 100 and 200 nm (Fig. 1), which corresponds to a typical growth rate of 2.5 nm per spray cycle. X ray diffraction and Raman analysis (not shown) show that the films have the orthorhombic InVO<sub>4</sub>-III crystal structure.<sup>10</sup> No traces of binary In- or V-oxide phases are observed. While trace amounts of another phase, presumably monoclinic InVO<sub>4</sub>-I, are difficult to avoid,<sup>10</sup> the spray deposition method allows synthesis of the orthorhombic phase at significantly lower temperatures than the 680°C required for conventional wet-chemical powder synthesis of InVO<sub>4</sub>-III.<sup>11</sup>

In order to be a useful photoanode material, InVO<sub>4</sub> should be photochemically stable in aqueous solutions. The stability of InVO<sub>4</sub> films deposited on quartz has been investigated for aqueous solutions with pH values between 1 and 14. For each pH value, the sample was immersed for 6 h, after which it was taken out for optical transmission measurements. Two sets of experiments were carried out, one in which the film was immersed in the dark, and the second set under continuous illumination with a 375-nm UV-LED array (also for 6 h). The resulting transmission measurements for the illuminated samples are shown in Fig. 2. Interestingly, nearly identical results are found in the absence of illumination. Between pH 3 and 14, no changes in the transmission are observed over the 6-h period, while a pH less than 2 results in the (partial) dissolution of the film. This shows that orthorhombic InVO<sub>4</sub>-III is stable between pH 3 and 14 in aqueous solutions. The similarity of the results found in the dark and under illumination

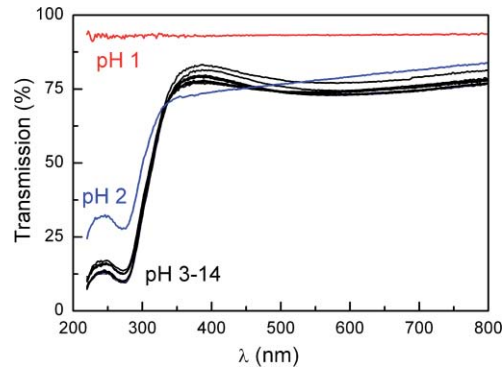


**Fig. 2** Optical transmission spectra of an InVO<sub>4</sub> film on quartz after successive 6 h exposures to 375-nm light in aqueous solutions of different pH.

is attributed to the absence of a closed electrochemical circuit. Without a catalytically active counter electrode to ensure efficient reduction kinetics and rapid consumption of photogenerated electrons, the system may quickly reach an equilibrium situation where the photo-generated holes recombine with the electrons before they reach the surface of InVO<sub>4</sub>. A more definitive evaluation of the stability of the material against photo-anodic decomposition would, therefore, require these experiments to be carried out in an electrochemical cell under actual operating conditions.

To determine the bandgap of the material, optical absorption measurements were carried out for a 180-nm InVO<sub>4</sub> film on quartz. The absorption coefficient is calculated using

$$\alpha = \frac{\ln(10)A}{L}. \quad (1)$$

Here,  $L$  is the film thickness and the absorbance  $A$  is defined as  $-\log[T/(1-R)]$ . The transmission ( $T$ ) and reflection ( $R$ ) coefficients cancel each other almost perfectly, and the absorption measured by placing the sample in the integrating sphere of the spectrometer did not vary more than a few percent from the value of  $(1-T-R)$ . A plot of the optical absorption coefficient as a function of wavelength is shown in Fig. 3(a). Although some visible light absorption between 400 and 450 nm is observed, it is much smaller than that observed for InVO<sub>4</sub> powders.<sup>6</sup> The reason for this will be discussed in more detail below. The bandgap of the material can be determined from the Tauc plots shown in Fig. 3(b). In view of the modest absorption at wavelengths  $>400$  nm, we interpret the  $(A \times h\nu)^{1/2}$  data as an indirect bandgap of 3.2 eV, combined with a sub-bandgap absorption that starts at 2.5 eV. The  $(A \times h\nu)^2$  curve also reveals a direct transition at 4.2 eV.

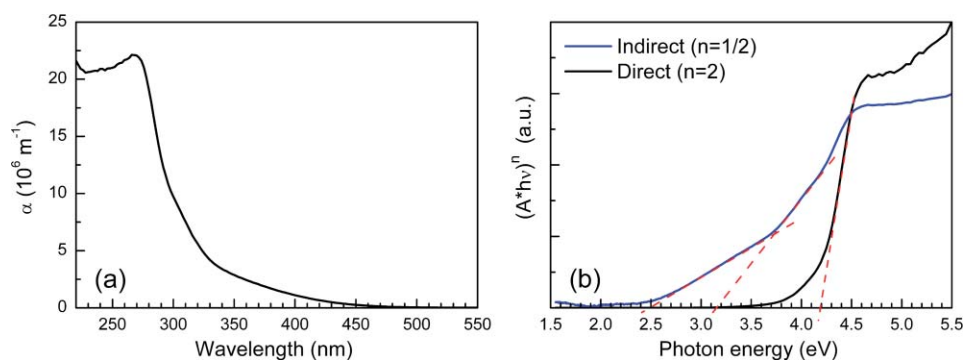


**Fig. 3** (a) Optical absorption coefficient of an InVO<sub>4</sub> film spray-deposited on quartz. (b) Tauc plots revealing the indirect and direct transitions of InVO<sub>4</sub>.

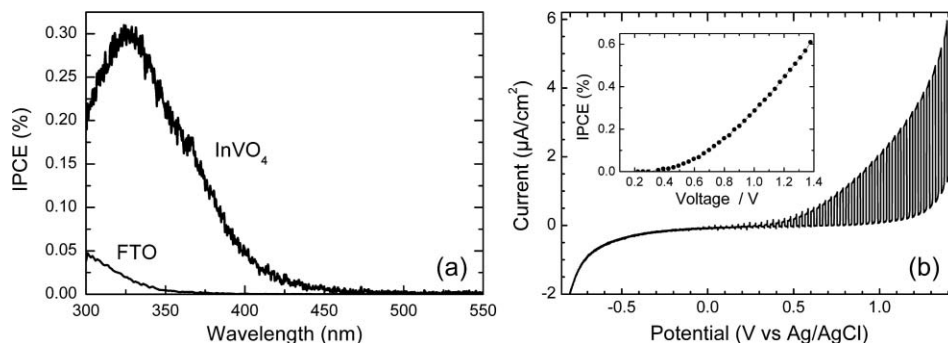


**Fig. 4** (a) Incident photon-to-current efficiency spectrum for InVO<sub>4</sub> on FTO measured at 0.8 V versus Ag/AgCl in a 0.1 M KOH solution (*pH* 13). (b) Chopped-light voltammogram using a 375 nm LED light source.

The indirect bandgap is significantly larger than the previously reported value of 1.9 to 2.0 eV for InVO<sub>4</sub>.<sup>6</sup> To see how this is reflected in the photoelectrochemical activity of the material, a photocurrent action spectrum was recorded for an InVO<sub>4</sub> film deposited on FTO glass. The corresponding incident photon-to-current efficiency (IPCE) is shown in Fig. 4(a). The photocurrent onset at about 450 nm ( $\sim 2.8$  eV) corresponds well with the optical absorption data. One noticeable difference is that the photocurrent maximum ( $\sim 325$  nm) is located at a longer wavelength than the optical absorption maximum [ $\sim 275$  nm, Fig. 3(a)]. This is probably due to a difference in penetration depth of the light, which corresponds to the film thickness for 325-nm light ( $\alpha^{-1} \approx 250$  nm) and decreases rapidly at shorter wavelengths. At 275 nm, the light only penetrates  $\sim 50$  nm which implies that the electrons have to travel an appreciable length to the back contact. This would indicate electron transport limitations in InVO<sub>4</sub>, although alternative explanations in terms of electronic structure effects cannot be ruled out.

Figure 4(a) shows a maximum external quantum efficiency (= IPCE) of 0.31% at  $\sim 330$  nm. Compared to other photoanode materials, this is a very low value that indicates extensive recombination. To investigate the origin of such a low value, the IPCE was also measured as a function of applied potential for a fixed wavelength of 375 nm. The results are shown in Fig. 4(b). Although the IPCE increases at potentials above 0.8 V versus Ag/AgCl, the value remains well below 1% up to 1.4 V. Several factors may be responsible for the poor photoresponse. Performance-limiting factors include slow charge transfer kinetics at the semiconductor/electrolyte interface, low electron- or hole-mobilities in the bulk, recombination at defect sites or grain boundaries, etc. The influence of hole transfer kinetics was investigated by comparing chopped-light (simulated AM1.5) voltammograms in solutions with and without methanol as a hole scavenger. As shown in Fig. 5, methanol has only a small influence on the observed photocurrent, indicating that slow oxidation kinetics are not responsible for the poor photoresponse of InVO<sub>4</sub>. No evidence for current-doubling is observed, in contrast to what is often found for TiO<sub>2</sub> (which has similar band positions).

To investigate the origin of the modest photoresponse, an electrochemical impedance spectroscopy study was carried out. While the details of this study are beyond the scope of the present paper, we briefly discuss our main findings here—a more extensive discussion can be found elsewhere.<sup>10</sup> The impedance study revealed a flatband potential of  $-0.04$  V versus reversible hydrogen electrode (RHE) ( $-1.01$  V versus Ag/AgCl at *pH* 13), consistent with previous observations of hydrogen evolution from InVO<sub>4</sub> powders.<sup>6</sup> In contrast, the photocurrent onset observed in Figs. 4 and 5 is at  $\sim 0.3$  V versus Ag/AgCl, i.e., at  $\sim 1.3$  V more positive potentials. Possible causes of such a high onset potential are recombination in the space charge layer or hole trapping at surface defects.<sup>10</sup> Hole accumulation at the surface can be ruled out as an explanation, since the MeOH experiments of Fig. 5 does not indicate slow oxidation kinetics. The impedance study further reveals that the system can be described by two parallel resistor-capacitor (RC)



combinations in series. One (RC) component corresponds to the bulk of the material, while the other one was found to describe the space charge present at the surface of the InVO<sub>4</sub> film. The RC time constant of the bulk is  $\sim 0.1$  to  $0.2$  ms, from which a bulk conductivity of  $\sim 4 \times 10^{-6} \Omega^{-1} \text{m}^{-1}$  was calculated. This is a relatively small value that appears to contradict the rather high donor density of  $6 \times 10^{19} \text{cm}^{-3}$  found from the analysis of the space charge capacitance. This contradiction has been attributed to the presence of donor states with energy levels that are deep in the bandgap.<sup>10</sup> Only a small fraction of these donors will be ionized, which explains the low bulk conductivity. This low conductivity may also explain the poor photoresponse of the InVO<sub>4</sub>. Another, perhaps more likely explanation is that the deep donors act as recombination centers for the photogenerated electron/hole pairs. This situation closely resembles that of TiO<sub>2</sub>, where the deliberate introduction of dopants (e.g., Cr or Fe) enhances the visible light response, but also leads to enhanced recombination. The communication of the deep donor states with free electrons in the conduction band is expected to be slow, which is consistent with the large time constant of the space charge component ( $\sim 10$  s). The constant capacitance at high frequencies resembles the behavior of an insulator and confirms the absence of ionized (shallow) donors in the material. In semiconductor terminology, the InVO<sub>4</sub> is in the ‘freeze-out’ regime.<sup>12</sup>

The presence of these deep donor states is believed to be responsible for the sub-bandgap absorption starting at 2.5 eV. In order to be consistent with the *n*-type behavior of InVO<sub>4</sub>, which is evident from the anodic nature of the photocurrent, the deep donor states would have to be located at 2.5 eV above the valence band. With a bandgap of 3.2 eV, this corresponds to a deep donor level at  $\sim 0.7$  eV below the conduction band. The proposed band diagram for InVO<sub>4</sub> is shown in Fig. 6. Since InVO<sub>4</sub> is in the freeze-out regime, the Fermi level is located halfway between the donor level and the conduction band minimum.<sup>12</sup> The diagram in Fig. 6(a) is clearly not able to explain the sub-bandgap photoresponse, since all the donor states are occupied and no optical transitions from the valence band to the donor state can occur. However, when immersed in water, partial depletion (i.e., ionization) of the donor states will occur. This leads to band bending and the formation of a depletion layer, as illustrated in Fig. 6(b). The ionized donor states can be filled through optical excitation of valence band electrons, which explains the sub-bandgap optical absorption of InVO<sub>4</sub>.

The width of the space charge region,  $W$ , was found to be less than 10 nm due to the high donor density.<sup>10</sup> From this, the sub-bandgap absorption is expected to be proportional to the surface area of InVO<sub>4</sub>. For powders prepared with a solid state reaction method, typical crystallite sizes of  $\sim 85$  nm have been reported,<sup>8</sup> which corresponds to a specific surface area of  $15 \text{m}^2/\text{g}$ . For the  $\sim 180$ -nm thick films that we have studied, the specific surface area is  $1.2 \text{m}^2/\text{g}$ , i.e., more than 10 times smaller. This large difference explains why the sub-bandgap absorption in InVO<sub>4</sub> powders<sup>6</sup> is much more pronounced than the absorption we observe for our thin films [Fig. 3(a)].

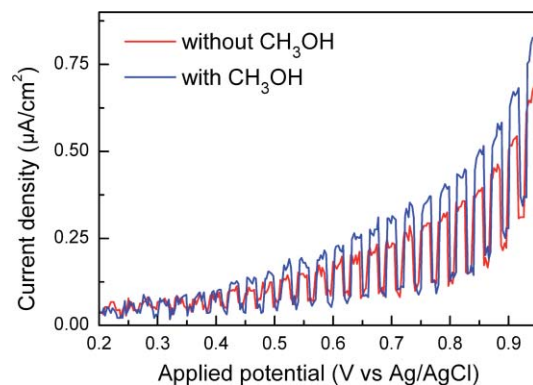


**Fig. 5** Chopped-light voltammogram using simulated AM1.5 light. A slightly higher photocurrent is observed in the presence of methanol, which acts as a hole scavenger.

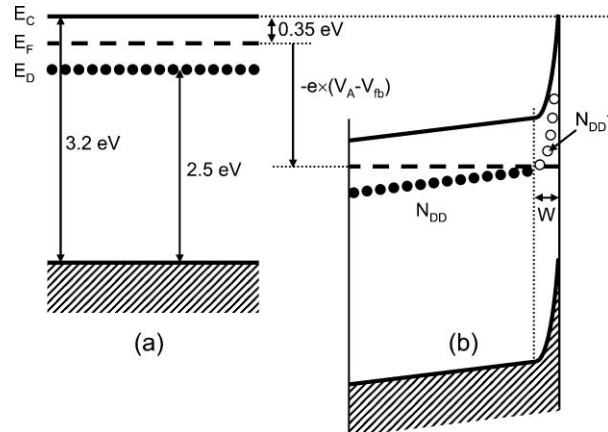


**Fig. 6** Illustration of deep donor states present in the bandgap of InVO<sub>4</sub>. (a) Flatband situation with all deep donor levels occupied. (b) At positive applied potentials, the deep donors in the space charge region are ionized.

To investigate the presence of deep donor states in more detail, photoluminescence (PL) measurements have been performed. Since the PL signal for thin films was too small to detect, the measurements were done on InVO<sub>4</sub> powders prepared by a straightforward solid state chemistry route. XRD and Raman measurements show these powders to be phase-pure orthorhombic InVO<sub>4</sub>-III, with no traces of any other phases present. The room-temperature PL spectra are shown in Fig. 7(a). The emission spectrum shows a single, clear peak at 2.16 eV upon excitation with 300-nm light. The excitation spectrum for this peak starts at about 3.2 to 3.3 eV, which is consistent with our previous assignment of 3.2 eV as the indirect bandgap of InVO<sub>4</sub>. The energy of the PL emission is significantly smaller than the 2.5 eV energy difference between the valence band and the deep donor state. We tentatively interpret this as donor-acceptor pair luminescence that involves the deep donor state and an acceptor state that is located at about  $\sim 0.3$  eV above the valence band. The energy diagram to explain the PL results is shown in Fig. 7(b).

Further improvement of InVO<sub>4</sub> photocatalysts requires a better understanding of the chemical nature of the deep donor states observed in this work. Although the presence of impurities cannot be excluded (a donor density of  $6 \times 10^{19} \text{ cm}^{-3}$  corresponds to a concentration of  $\sim 0.05\%$ ), deviations from the ideal In:V ratio of 1:1 seem a more likely explanation. For example, excess indium ions may act as donors when incorporated on interstitial sites. Using the standard

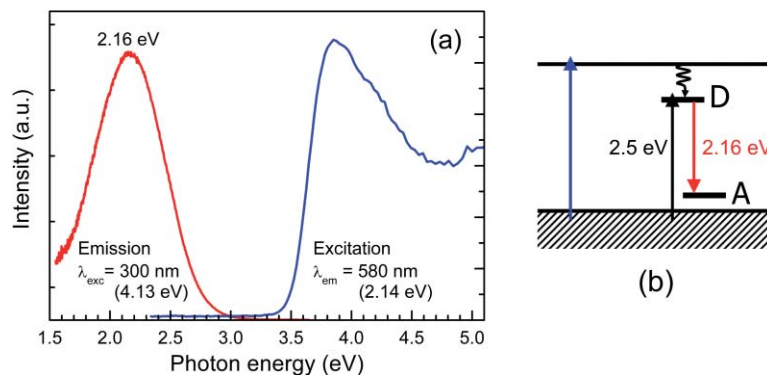
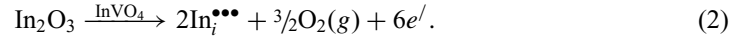


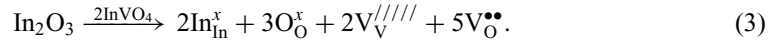
**Fig. 7** (a) Room-temperature photoluminescence emission and excitation spectra for InVO<sub>4</sub> powder. (b) Energy diagram that illustrates how a donor-acceptor pair can explain the observed emission spectrum.



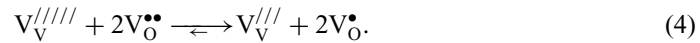
Kröger–Vink notation,<sup>13</sup> this reaction can be written as



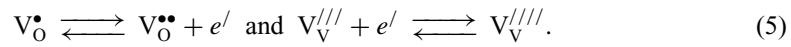
However, no acceptor species are formed during this reaction, and it cannot explain the PL results in a satisfactory manner. A more likely mechanism is that an excess of indium results in ionic compensation through the formation of vanadium vacancies:



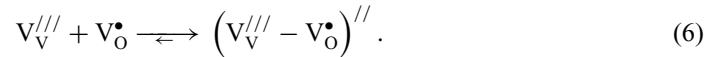
The presence of such highly charged vanadium vacancies is extremely unlikely, and this reaction will therefore be followed by partial charge transfer from the vanadium vacancies to the oxygen vacancies, e.g.,



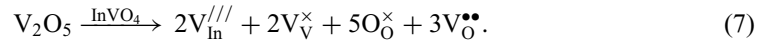
The singly-ionized oxygen vacancy and the trivalent vanadium vacancy may be the deep donor and the acceptor species, respectively, responsible for the photoluminescence response. The ionization of these species can be written as<sup>14</sup>



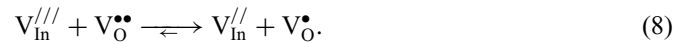
In order for donor-acceptor pair luminescence to occur, the donor and acceptor species should be in a situation close to each other. At high defect concentrations, such a close proximity is in fact quite likely to occur through the formation of defect associates:



An alternative defect mechanism may involve an excess of vanadium, and the formation of indium and oxygen vacancies as the acceptor and deep donor species:



Again, partial charge transfer from the metal vacancy can result in singly-ionized oxygen vacancies as deep donors, while the indium vacancies now act as acceptor species:



As outlined above, the ionization energy of the deep donor is  $\sim 0.7$  eV. Oxygen vacancies usually have ionization energies between 0.5 and 2.0 eV, whereas somewhat smaller values are usually reported for cation interstitials.<sup>13</sup> This is consistent with our tentative assignment as oxygen vacancies being the source of the deep donors, although a more definite assignment requires further investigation and is beyond the scope of this paper.

Finally, we point out that actual deviations from the ideal molecularity are impossible to avoid in wet-chemical processes. Although the In<sub>2</sub>O<sub>3</sub>–V<sub>2</sub>O<sub>5</sub> phase diagram indicates that InVO<sub>4</sub> is a line compound (cf. Fig. 8),<sup>15</sup> deviations as small as 0.05% (which corresponds to a donor density of  $10^{19}$  cm<sup>-3</sup>) may easily occur. Even if segregation of a binary In- or V-oxide occurs, the concentrations will be very low and may be impossible to observe with x ray diffraction or Raman spectroscopy. This is especially true for wet chemical synthesis methods, in which the ions are mixed on a molecular level and any segregated binary oxide phase will be present as finely dispersed amorphous precipitates or nanocrystallites.

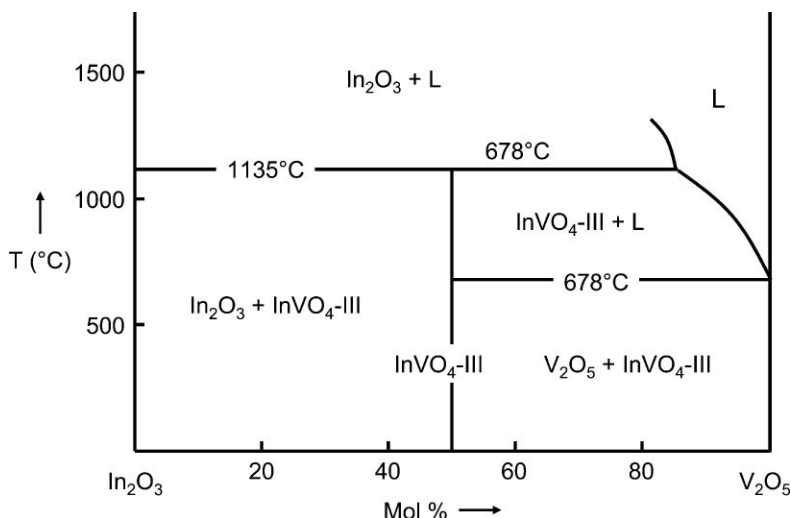


Fig. 8  $\text{In}_2\text{O}_3$ - $\text{V}_2\text{O}_5$  phase diagram [adapted from Touboul et al. (Ref. 16)].

## 4 Conclusions

With an indirect bandgap of 3.2 eV,  $\text{InVO}_4$  can be used as a photocatalyst in the UV range of the spectrum. Its main features are the high stability over a wide  $\text{pH}$  range (3 to 11), and the previously reported flatband potential of  $-0.04$  V versus RHE that enables hydrogen evolution.<sup>10</sup> The presence of deep donor states in the material leads to visible light absorption at photon energies  $>2.5$  eV. However, only ionized donors in the space charge region are optically active. If the visible light absorption of  $\text{InVO}_4$  is to be exploited, one needs to optimize the number of donors. A large donor concentration is favorable in terms of the number of optical absorption centers, but it also decreases the space charge width in which the donors are ionized. A striking feature of the  $\text{InVO}_4$  films studied here is the apparent absence of shallow donors, which may lead to electron transport limitations in the bulk of the material. Combined with the fact that visible light absorption mainly occurs close to the surface of the material, a nanosized powder appears to be optimum morphology for photocatalytic applications based on  $\text{InVO}_4$ . Finally, we point out that the formation of point defects upon deviations from the ideal stoichiometry is a general phenomenon in ternary and more complex metal oxides. The implications of our deep donor model may therefore extend to other complex metal oxide photoanodes, even though the energies and probabilities of the sub-bandgap optical transitions may vary.

## Acknowledgments

The authors gratefully acknowledge financial support from the “Sustainable Hydrogen” Programme at TU Delft. RvdK acknowledges the Netherlands Organization for Scientific Research (NWO) for a VENI grant which made part of these investigations possible. We thank Mr. R. Abellon from the Opto-electronic Materials group at the Chemical Engineering Department for help with the optical absorption and photoluminescence measurements.

## References

1. R. van de Krol, Y. Q. Liang, and J. Schoonman, “Solar hydrogen production with nanostructured metal oxides,” *J. Mater. Chem.* **18**, 2311–2320 (2008).
2. S. Licht, B. Wang, S. Mukerji, T. Soga, M. Umeno, and H. Tributsch, “Efficient solar water splitting, exemplified by  $\text{RuO}_2$ -catalyzed  $\text{AlGaAs/Si}$  photoelectrolysis,” *J. Phys. Chem. B* **104**, 8920–8924 (2000).

3. M. Grätzel, "Photoelectrochemical cells," *Nature (London)* **414**, 338–344 (2001).
4. A. Kay, I. Cesar, and M. Grätzel, "New benchmark for water photooxidation by nanostructured alpha-Fe<sub>2</sub>O<sub>3</sub> films," *J. Am. Chem. Soc.* **128**, 15714–15721 (2006).
5. B. D. Alexander, P. J. Kulesza, L. Rutkowska, R. Solarz, and J. Augustynski, "Metal oxide photoanodes for solar hydrogen production," *J. Mater. Chem.* **18**, 2298–2303 (2008).
6. J. H. Ye, Z. G. Zou, M. Oshikiri, A. Matsushita, M. Shimoda, M. Imai, and T. Shishido, "A novel hydrogen-evolving photocatalyst InVO<sub>4</sub> active under visible light irradiation," *Chem. Phys. Lett.* **356**, 221–226 (2002).
7. S. C. Zhang, C. Zhang, H. P. Yang, and Y. F. Zhu, "Formation and performances of porous InVO<sub>4</sub> films," *J. Solid State Chem.* **179**, 873–882 (2006).
8. L. W. Zhang, H. B. Fu, C. Zhang, and Y. F. Zhu, "Synthesis, characterization, and photocatalytic properties of InVO<sub>4</sub> nanoparticles," *J. Solid State Chem.* **179**, 804–811 (2006).
9. M. Oshikiri, M. Boero, J. Ye, F. Aryasetiawan, and G. Kido, "The electronic structures of the thin films of InVO<sub>4</sub> and TiO<sub>2</sub> by first principles calculations," *Thin Solid Films* **445**, 168–174 (2003).
10. C. S. Enache, D. Lloyd, M. R. Damen, J. Schoonman, and R. van de Krol, "Photoelectrochemical properties of thin-film InVO<sub>4</sub> photoanodes: The role of deep donor states," *J. Phys. Chem. C* **113**, 19351–19360 (2009).
11. M. Touboul, K. Melghit, P. Benard, and D. Louer, "Crystal-Structure of a Metastable Form of Indium Orthovanadate, InVO<sub>4</sub>-I," *J. Solid State Chem.* **118**, 93–98 (1995).
12. R. F. Pierret, *Advanced Semiconductor Fundamentals*, Addison-Wesley Reading, MA (1989).
13. F. A. Kröger, *The Chemistry of Imperfect Crystals*, North-Holland Publishing Co., Amsterdam (1964).
14. Y.-M. Chiang, D. Birnie III, and D. W. Kingery, *Physical Ceramics*, Wiley, New York (1997).
15. M. Touboul and A. Popot, "Control of purity and crystallinity of AlVO<sub>4</sub>, CrVO<sub>4</sub>, FeVO<sub>4</sub>, InVO<sub>4</sub>, YVO<sub>4</sub>, NdVO<sub>4</sub> compounds by DTA," *J. Thermal Anal.* **31**, 117–124 (1986).
16. M. Touboul, K. Melghit, and P. Benard, "Synthesis by Chimie-Douce and characterization of indium vanadates," *Eur. J. Solid State Inorg. Chem.* **31**, 151–161 (1994).

**Roel van de Krol** received his MSc and PhD degrees in materials science from Delft University of Technology in 1995 and 2000, respectively, after which he was a postdoctoral fellow at the Massachusetts Institute of Technology. In 2001 he returned to Delft University of Technology where he is currently an assistant professor. His current research activities focus on nanostructured metal oxide semiconductors for solar energy conversion and photocatalysis.

**Julie Ségalini** received her MSc degree from the European Erasmus Mundus program on Materials for Energy Storage and Conversion (MESCC) in 2008. She is currently a PhD student at Paul Sabatier University in Toulouse, France, where she works on materials for supercapacitors.

**Cristina S. Enache** received her MSc degree from the University of Transylvania in Brasov, Romania, and started her PhD studies at Delft University of Technology in 2002. Since 2008 she has worked as a process engineer at Scheuten Solar in Venlo, The Netherlands.